Immunoliposome-mediated drug delivery to *Plasmodium*-infected and non-infected red blood cells as a dual therapeutic/prophylactic antimalarial strategy

Ernest Moles [a,b,c], Patricia Urbán [a,b,c], María Belén Jiménez-Díaz [d], Sara Viera-Morilla [d], Iñigo Angulo-Barturen [d], Maria Antònia Busquets [c,e], and Xavier Fernàndez-Busquets [a,b,c,*]

[a] Nanomalaria Group, Institute for Bioengineering of Catalonia (IBEC), Baldiri Reixac 10-12, ES-08028 Barcelona, Spain
[b] Barcelona Institute for Global Health (ISGlobal, Hospital Clínic-Universitat de Barcelona), Rosselló 149-153, ES-08036 Barcelona, Spain
[c] Nanoscience and Nanotechnology Institute (IN2UB), University of Barcelona, Martí i Franquès 1, ES-08028 Barcelona, Spain
[d] Tres Cantos Medicines Development Campus, GlaxoSmithKline, Severo Ochoa 2, ES-28760 Tres Cantos, Spain
[e] Departament de Fisicoquímica, Facultat de Farmàcia, University of Barcelona, Av. Joan XXIII, s/n, ES-08028 Barcelona, Spain
*e-mail: xfernandez_busquets@ub.edu

Abstract
One of the most important factors behind resistance evolution in malaria is the failure to deliver sufficiently high amounts of drugs to early stages of *Plasmodium*-infected red blood cells (pRBCs). Despite having been considered for decades as a promising approach, the delivery of antimalarials encapsulated in immunoliposomes targeted to pRBCs has not progressed towards clinical applications, whereas *in vitro* assays rarely reach drug efficacy improvements above 10-fold. Here we show that encapsulation efficiencies reaching >96% are achieved for the weak basic drugs chloroquine (CQ) and primaquine using the pH gradient loading method in liposomes containing neutral saturated phospholipids. Targeting antibodies are best conjugated through their primary amino groups, adjusting chemical crosslinker concentration to retain significant antigen recognition. Antigens from non-parasitized RBCs have also been considered as targets for the delivery to the cell of drugs not affecting the erythrocytic metabolism. Using this strategy, we have achieved unprecedented complete nanocarrier targeting to early intraerythrocytic stages of the malaria parasite for which there is a lack of specific extracellular molecular tags. Immunoliposomes studded with monoclonal antibodies raised against the erythrocyte surface protein glycophorin A were capable of targeting 100% RBCs and pRBCs at the low concentration of 0.5 μM total lipid in the culture, with >95% of added liposomes retained on cell surfaces. When exposed for only 15 min to *Plasmodium falciparum in vitro* cultures of early stages, free CQ had no significant effect on the viability of the parasite up to 200 nM, whereas immunoliposomal 50 nM CQ completely arrested its growth. *In vivo* assays in mice showed that immunoliposomes cleared the pathogen below detectable levels at a CQ dose of 0.5 mg/kg, whereas free CQ administered at 1.75 mg/kg was, at most, 40-fold less efficient. Our data suggest that this significant improvement is in part due to a prophylactic effect of CQ found by the pathogen in its host cell right at the very moment of invasion.

Keywords: immunoliposomes; malaria; nanomedicine; *Plasmodium*; targeted drug delivery.

Chemical compounds studied in this article: Chloroquine (PubChem CID: 2719); Primaquine (PubChem CID: 4908); DSPC (PubChem CID: 94190); DOPC (PubChem CID: 6437081); Cholesterol (PubChem CID: 5997); Maleimide (PubChem CID: 10935); SATA (PubChem CID: 127532); Pyranine (PubChem CID: 61389); Hoechst 33342 (PubChem CID: 1464).

1. Introduction

The majority of chemotherapeutic approaches against malaria are targeted at the *Plasmodium* stages infecting red blood cells (RBCs), which are responsible for all symptoms and pathologies of the disease [1]. Because of the amphiphilicity of most current antimalarial drugs, they are extensively distributed into body tissues after administration and can be rapidly metabolized in the liver [2]. In the blood vessels, antimalarial drugs circulate mainly associated to plasma proteins [3] and are usually quickly removed from circulation, presenting relatively short half-lives from less than one hour to few hours [2]. These shortcomings are usually compensated through administration of increased doses, in a delicate narrow edge between high overall amounts causing toxic side effects [4] and low local concentrations inducing resistance evolution in most malaria-endemic countries [5].

Drugs specifically targeted to parasitized RBCs (pRBCs) would benefit from a reduction in the body distribution volume, lasting longer in the bloodstream while avoiding degradation, and increasing exposure of the pathogen to lethal doses. Liposomal nanovectors bearing cell-specific antibodies on their surfaces (immunoliposomes, iLPs) have been widely considered as chemotherapeutic drug carriers due to their non-toxic and biodegradable character [6], but they have not progressed yet towards a working strategy for malaria therapeutics. Pioneering assays to treat *Plasmodium berghei* infections in mice focused on the encapsulation of the antimalarial drug chloroquine into liposomes (LPs) and iLPs functionalized with antibodies against RBCs and pRBCs [7-9]. Drug efficacy was significantly improved upon encapsulation, especially when targeted towards pRBCs, and after treatment with iLPs, mice exhibited lower parasitemias and longer survival times even with drug-resistant strains. These improvements were attributed to the specific interaction of targeting antibodies with RBCs/pRBCs and to the efficient incorporation of LP contents into the cells, although liposomal models were poorly characterized with no direct evidence for LP internalization and absence of encapsulated drug stability and release kinetics analyses. Moreover, because all these studies were done in murine malarias, there was a lack of data for human-infecting parasites, particularly for the deadliest species, *Plasmodium falciparum*.

Recently, *in vitro* assays in *P. falciparum* have shown that LPs functionalized with pRBC-specific antibodies can specifically recognize target cells vs. non-infected erythrocytes in less than 90 min [10]. The short time required to achieve complete specificity was an encouraging result that opened good perspectives regarding the development of a rapid delivery nanovector capable of competing with LP clearance from blood by macrophages and the liver [11]. Nevertheless, this good targeting has not been able to provide improvements in drug efficacy above 10-fold [12], and parasitemia could not be completely eliminated from the cultures. *In vivo* assays in mice grafted with human erythrocytes and subsequently infected with *P. falciparum* [13] showed that some iLP-encapsulated antimalarials had a clearly improved efficacy (Fig. 1A). However, as in *in vitro* assays, *Plasmodium* parasites could not be completely cleared despite the continuous presence of iLPs in the blood of mice during the entire length of four-day tests (Fig. 1B).

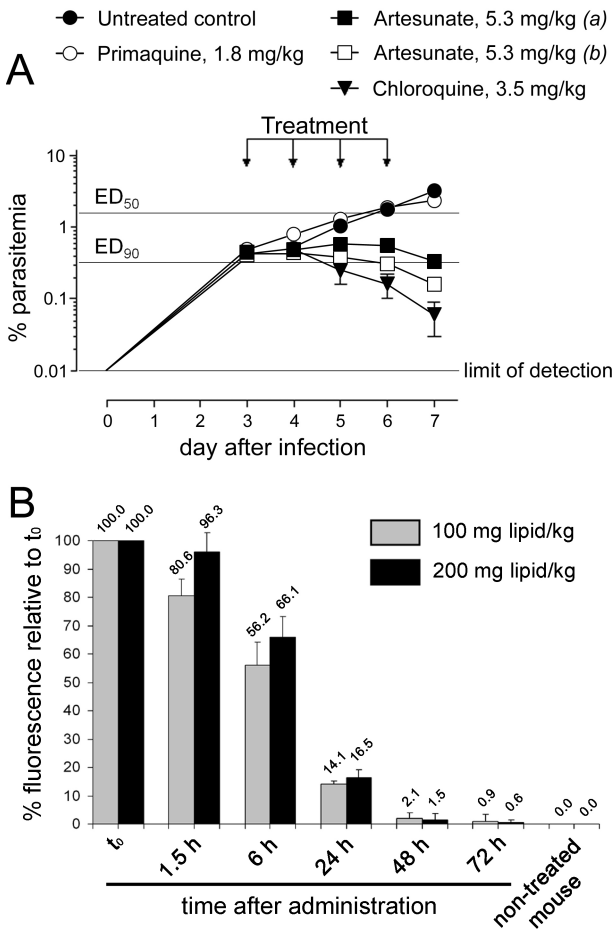

Fig. 1. (A) 4-day test in female immunodeficient mice engrafted with human erythrocytes and infected i.v. with *P. falciparum*. The different curves correspond to drug-containing iLPs functionalized with the pRBC-specific antibody *BM1234* as previously described [10]. *(a)* and *(b)* correspond to artesunate-containing iLPs where the drug was added, respectively, to the lipid mixture before evaporation of the solvent, or to the aqueous buffer added to the dry lipids to form LPs. (B) Residence time in the bloodstream of mice of rhodamine-labeled LPs with the same lipid composition as in (A).

Often, the particularities of malaria pathophysiology have not been sufficiently considered when designing iLPs for targeted antimalarial drug delivery. Most drugs used in the treatment of malaria are amphiphilic compounds whose capacity to solubilize in both aqueous and organic phases allows them to easily cross lipid bilayers, which complicates their liposomal encapsulation. Therefore, special liposome formulations including saturated long-chain phospholipids with elevated phase transition temperatures (>37 °C) together with low amounts of cholesterol are crucial components required to avoid the otherwise quick leakage of small molecules [14]. In addition, since lipid bilayers are highly impermeable to ionized species, working at the adequate pH is paramount to sustain a proton gradient and attain higher liposomal drug loads. Other factors to be taken into account are the nature, location, and abundance of markers on pRBC surfaces: although *Plasmodium* proteins are found in the plasma membrane of pRBCs [15], those currently known are highly variable or have a low abundance [16]. Given this scarcity of adequate antigens exposed on pRBCs, essential parameters that will be determinant in the capacity of iLPs to recognize and bind target cells are a careful selection of sufficiently specific antibodies, the way they are crosslinked to lipids, and their numbers on the liposome surface. Since RBCs have very poor endocytic processes [17], once iLPs are docked to them delivery of cargo into the cell has been proposed to occur through a membrane fusion process [7,10,18,19]. Nevertheless, considering the lack of strong evidence and the poor characterization of this fusion process using RBCs and pRBCs as targeted cells, alternative mechanisms of interaction should be considered. These include, but are not limited

to, the stable adsorption on the target cell surface or the entry through the tubulovesicular network (TVN) [17] and other modifications suffered by erythrocyte membranes when the cell has been parasitized by *Plasmodium*.

Here we have dissected the different iLP parts to propose a rational design strategy for the administration of lethal amounts of drugs to the intraerythrocytic pathogen. The results presented can significantly contribute to developing new and optimized targeted drug delivery approaches against malaria based on a dual and simultaneous (i) therapeutic activity on pRBCs and (ii) prophylactic effect against erythrocyte infection by *Plasmodium*.

2. Materials and methods

2.1. Materials

Except where otherwise indicated, reactions were performed at room temperature (20 °C), and reagents were purchased from Sigma-Aldrich Corporation (St. Louis, MO, USA). The lipids (all ≥99% purity according to thin layer chromatography analysis) 1,2-dioleoyl-*sn*-glycero-3-phosphocholine (DOPC), 1,2-distearoyl-*sn*-glycero-3-phosphocholine (DSPC), 1,2-dioleoyl-*sn*-glycero-3-phosphoethanolamine-N-[4-(p-maleimidophenyl)butyramide] (MPB-PE), 1,2-distearoyl-*sn*-glycero-3-phosphoethanolamine-N-[maleimide(polyethylene glycol)-2000] (DSPE-PEG2000-Mal), 1,2-dioleoyl-*sn*-glycero-3-phosphoethanolamine-N-[lissamine rhodamine B sulfonyl] (DOPE-Rho), and 1,2-dioleoyl-*sn*-glycero-3-phosphoethanolamine-N-[methoxy(polyethylene glycol)-2000] (PE-PEG2000) were purchased from Avanti Polar Lipids Inc. (Alabaster, AL, USA). Mouse monoclonal IgG anti-human GPA SM3141P, rabbit polyclonal IgG anti-human GPA AP05437PU-N, mouse monoclonal anti-HRP2 AM01200PU-N, and mouse monoclonal IgM BM1234 were purchased from Acris Antibodies, Herford, Germany.

2.2. Preparation of LPs and encapsulation of drugs

LPs with a basic formulation of neutrally charged unsaturated (DOPC:cholesterol, 80:20) or saturated (DSPC:cholesterol, 90:10) phospholipids were prepared by the lipid film hydration method [20]. Briefly, stock lipids in chloroform were mixed and dissolved in chloroform:methanol (2:1, v/v) in a round-bottomed flask. Organic solvents were removed by rotary evaporation under reduced pressure at 37 °C, in a progressive vacuum range from −20 to −70 mmHg, to yield a thin lipid film on the flask bottom and walls. For passive drug encapsulation, the dried lipids were then hydrated to 10 mM total lipid in 10 mM phosphate buffer, pH 6.5, containing the desired drug/molecule to encapsulate and osmotically adjusted to 320 mOsm/kg (isotonic with *P. falciparum* growth medium) by addition of 5 M NaCl. Multilamellar LPs were formed by 3 cycles of constant vortexing followed by bath sonication for 3 minutes each, and downsized to unilamellar vesicles by extrusion through 200 nm polycarbonate membranes (Poretics, Livermore, CA, USA) in an extruder device (LiposoFast, Avestin, Ottawa, Canada). Throughout the lipid film hydration and downsizing processes samples were maintained above lipid transition temperature. LP size was determined by dynamic light scattering using a Zetasizer NanoZS90 (Malvern Ltd, Malvern, UK). Unencapsulated material was removed by buffer exchange in 7-kDa Zeba™ spin desalting columns (Thermo Fisher Scientific, Inc.) using isotonic phosphate buffered saline (PBS) at the desired pH (7.5 unless otherwise indicated). Finally, liposomal suspensions to be used in assays with live cells were sterile filtered through 0.22 µm pore size polyvinylidene difluoride (PVDF) filters (Millex-GV Syringe Filter Units, 4 mm, Millipore). Active encapsulation by the pH gradient method was done following an adaptation of established protocols [21], substituting saturated DSPC for unsaturated DOPC to obtain a lipid bilayer capable of sustaining a proton gradient. LPs were prepared in 200 mM citrate buffer at pH 4.0 and buffer exchanged with isotonic PBS containing 10 mM ethylenediaminetetraacetic acid (EDTA) in order to establish a pH gradient across the LP membrane. One volume of drug was then mixed with ten volumes of LPs to reach final

concentrations of 500 µM chloroquine (CQ) and 1 mM primaquine (PQ) and the mixture was stirred for 30 min at room temperature before immediately proceeding, when required, to antibody coupling.

2.3. Generation of polyclonal antibodies against MAHRP1$_{21-40}$ peptide

MAHRP1$_{21-40}$ (ADVPTEGMDVPFGFFDKNTL) was synthesized (Peptide Synthesis Service, Scientific and Technological Centers, University of Barcelona) with an additional cysteine at the carboxy terminal end. Immunization of rabbits was done at the facilities of the Animal Experimentation Services (University of Barcelona) following standard protocols. Serum antibodies were purified by affinity chromatography using the corresponding peptides immobilized on agarose beads (SulfoLink Kit, Pierce Biotechnology, Rockford, IL, USA), assayed by Enzyme-Linked ImmunoSorbent Assay (ELISA), and finally stored at −20 °C.

2.4. Generation of iLPs

Freshly prepared maleimide-containing LPs were conjugated with thiolated antibodies following established protocols [22]. The generation of sulfhydryl groups in antibodies was performed through three alternative approaches: (i) Half-antibodies bearing free thiols generated by reduction with 2-mercaptoethylamine-HCl (MEA, Thermo Fisher Scientific, Inc.) were obtained as described previously [10]. (ii) Reactive aldehyde groups (CHO) were generated in the carbohydrate moieties of antibody (Ab) Fc regions by oxidation in PBS containing 5 mM sodium periodate (1 h, protected from light) [23]. Oxidized antibodies were then recovered by buffer exchange in PBS, pH 7.2, and conjugated by hydrazone linkage through a 2-h incubation with a 150-fold molar excess of freshly dissolved 3-(2-pyridyldithio)propionyl hydrazide crosslinker (PDPH, Thermo Fisher Scientific, Inc.). The number of reactive aldehyde groups available (ca. 2/Ab) was quantified before PDPH conjugation by incubation of oxidized antibodies with Lucifer Yellow CH fluorescent dye, as described previously [24]. Excess of crosslinker was removed by buffer exchange in SAS buffer (100 mM sodium acetate, 50 mM NaCl, pH 4.4) and thiol groups were finally exposed through pyridyldithiol group cleavage by addition of 25 mM dithiothreitol (DTT) and incubation for 20 min. (iii) For the non-oriented binding through primary amino groups, antibodies in PBS were reacted for 30 min with a 10× to 100× molar excess relative to antibody molecules of the crosslinker N-succinimidyl S-acetylthioacetate (SATA, Thermo Fisher Scientific, Inc.) freshly dissolved in dimethyl sulfoxide. Unreacted SATA was removed by buffer exchange in PBS and protected thiols in SATA-conjugated antibodies were exposed by addition of 50 mM hydroxylamine and 2.5 mM EDTA. After thiolation, antibodies were recovered by buffer exchange in PBS supplemented with 10 mM EDTA and the number of available sulfhydryl groups was determined by reaction with 5,5'-dithio-bis-(2-nitrobenzoic acid) (DTNB, Thermo Fisher Scientific, Inc.). 400 µg DTNB/ml were added to the thiolated antibody solution, and after 20 min the formation of 2-nitro-5-thiobenzoic acid was quantified by measuring its absorbance at 412 nm. Finally, coupling of freshly thiolated antibodies to freshly prepared maleimide-containing LPs was done overnight (12 to 15 h) in PBS supplemented with 10 mM EDTA. Unbound antibodies were removed by ultracentrifugation (150,000 *g*, 1 h, 4 °C), maintaining the same tonicity and LP concentration (10 mM lipid) during the whole process. For the intercalation of a polyethylene glycol (PEG) linker between LP and antibody, DSPE-PEG2000-Mal was substituted for MPB-PE in the LP formulation. Pelleted iLPs were taken up in PBS and stored at 4 °C for up to one month before being used. Antibody coupling was quantitatively assessed by protein determination with the DC™ Protein Assay (Bio-Rad). Coupling efficiency (%) was determined as the fraction of LP-bound antibody relative to total antibody added; the number of bound antibodies per LP was determined considering an IgG molecular mass of 150 kDa and the theoretical lipid content of a LP 170 nm in diameter composed solely of phosphatidylcholine [25]. For qualitative SDS-polyacrylamide gel electrophoresis (PAGE) coupling analysis, supernatant and pelleted iLP samples were heated at 90 °C for 3 min in 1×

Laemmli sample buffer, supplemented with 355 mM 2-mercaptoethanol, and electrophoresed in 7.5% SDS-polyacrylamide gels using the Mini Protean II System (Bio-Rad). For silver staining of gels [26], they were fixed (40% ethanol, 10% acetic acid) during 30 min and activated (30% ethanol, 41 mg/ml sodium acetate, 1.27 mg/ml sodium thiosulfate) for 30 min. After washing with deionized water (Milli-Q system, Millipore), gels were stained (1 mg/ml silver nitrate, 0.02% formaldehyde) for 40 min and protein bands were developed (25 mg/ml sodium carbonate, freshly prepared 0.01% formaldehyde). Finally, the reaction was terminated by addition of 1% acetic acid and gels were stored in 10% glycerol solution.

2.5. Quantification of drugs and fluorescent dyes in LP samples

Encapsulated CQ and PQ were quantified by measuring their respective absorbances at 342 and 352 nm after LP (0.5 mM lipid) disruption by treatment with 2% v/v Triton X-100 in PBS, subtracting the lecture of drug-free LPs. Encapsulated fluorescent dye quantification was performed by fluorescence analysis (Synergy HT Multi-Mode Microplate Reader, BioTEK) of pyranine ($\lambda_{ex/em}$ = 488/520 nm), and of rhodamine-conjugated lipid (DOPE-Rho; $\lambda_{ex/em}$ = 530/590 nm). Encapsulation efficiency (EE, %) represents the encapsulated fraction relative to total compound added to the LP-containing solution. High performance liquid chromatography-tandem mass spectrometry (HPLC-MS/MS) was used to quantify CQ concentrations below the detection limit of UV-Vis spectroscopy (20 nM and 2 µM CQ detection limits for HPLC-MS/MS and UV-Vis spectroscopy, respectively), according to established protocols [12]. The release rate from LPs of encapsulated CQ and PQ was determined at selected time points by drug quantification in the supernatants and corresponding pelleted LPs obtained after ultracentrifugation (100,000 *g*, 45 min, 4 °C). Release rates were expressed as the percentage of drug in the supernatant relative to the total drug present in the sample. All experimental values are represented as mean ± SD for 3 replicates.

2.6. P.falciparum in vitro culture and growth inhibition assays

P.falciparum strain 3D7 was grown *in vitro* in group B human erythrocytes using previously described conditions [27]. Parasites (thawed from glycerol stocks) were cultured at 37 °C in Petri dishes with RBCs at 3% hematocrit in Roswell Park Memorial Institute (RPMI) complete medium containing Albumax II (RPMI-A, Invitrogen), supplemented with 2 mM L-Glutamine, under a gas mixture of 92% N_2, 5% CO_2, and 3% O_2. Synchronized cultures in early ring stages (0-24 h post-invasion) were obtained by 5% sorbitol lysis [28]. Late-form trophozoite and schizont stages (24-36 h and 36-48 h post-invasion, respectively) were purified in 70% Percoll (GE Healthcare) [28,29]. Parasitemia was determined by microscopic counting of blood smears fixed briefly with methanol and stained with Giemsa (Merck Chemicals) diluted 1:10 in Sorenson's buffer, pH 7.2, for 10 min. For culture maintenance, parasitemia was kept below 5% late forms and 10% early forms by dilution with freshly washed RBCs and the medium was changed every 1-2 days. For *P.falciparum in vitro* growth inhibition assays, cultures synchronized (>95%) in early ring or late form stages were brought to 4% hematocrit and 1% parasitemia by dilution with fresh RBCs. After adding one culture volume of 2× concentrated drug solution in RPMI-A, cultures were incubated for 15 min in 2-ml Petri dishes under orbital stirring, transferred to microcentrifuge tubes, and cells were spun down, finally replacing the medium with fresh RPMI-A. Unless otherwise specified, the data presented throughout the manuscript refer to samples containing 2% hematocrit. The resulting cell suspension was then seeded on 96-well plates (Merck Chemicals) and further incubated for a complete 48-h growth cycle under the conditions described above. For growth inhibition determination, samples were diluted 1:100 in PBS, and the nuclei of pRBCs (the only nucleated cells present in the culture) were stained by addition of 0.1 µM Syto11 (Thermo Fisher Scientific, Inc.) in the final mixture before proceeding to flow cytometry analysis.

2.7. Protein expression analysis throughout the 48-h intraerythrocytic cycle

For the analysis of MAHRP-1 (*BM1234* antigen) and HRP2 protein expression throughout the whole intraerythrocytic cycle of *P. falciparum*, tightly synchronized cultures (0-5 h range, 8% parasitemia) were obtained using a combination of 70% Percoll and 5% sorbitol (5 h after release of merozoites) stage-selection methods as described above. Culture samples corresponding to 3 µl pRBCs were obtained at the following post-infection timepoints: 12 h, 20 h (rings); 26 h, 35 h, 38 h (trophozoites); 42 h, 44 h and 46 h (schizonts). Protein expression was analyzed by subcellular detergent fractionation (see below) and SDS-PAGE/Western blot, as previously described [10], using the primary monoclonal antibodies *BM1234* (2 µg/ml) and anti-HRP2 (0.5 µg/ml), and as secondary antibody goat anti-mouse IgG horseradish peroxidase-conjugated (1 µg/ml, Thermo Fisher Scientific, Inc.).

2.8. Fluorescence microscopy

Antigen localization in fixed cells by fluorescence confocal microscopy was done according to established protocols [10]. Briefly, air-dried blood smears were fixed in 1% formaldehyde and cell membranes were labeled with 3.3 µg/ml wheat germ agglutinin-tetramethylrhodamine (WGA-Rho) conjugate (Molecular Probes, Eugene, OR, USA). Slides were then incubated in the presence of 20 µg/ml of the mouse monoclonal antibodies *BM1234* or anti-HRP2, and the rabbit polyclonal antibodies anti-PfEMP1 (raised against the conserved C-terminal domain, gently provided by Dr. Alfred Cortés) and MAHRP1$_{21\text{-}40}$, followed by incubation in the presence of 6.7 µg/ml of the corresponding Alexa Fluor® secondary antibodies goat anti-mouse AF488 or AF660, or goat anti-rabbit AF488 (all from Molecular Probes), and of 1 µg/ml 4′ 6-diamino-2-phenylindole (DAPI, Invitrogen) for nuclei staining. All antibody treatments were done for 1 h in the presence of 0.75% w/v bovine serum albumin as blocking agent. Finally, slides were washed with PBS, mounted with ProLong® Gold antifade reagent (Molecular Probes), and examined with a Leica TCS SP5 laser scanning confocal microscope as described [10].

For immunofluorescence assays with live cells of the targeting efficiency of free antibodies and iLPs, *P. falciparum* cultures at 5% parasitemia were washed 3× with RPMI-A (700 *g*, 2 min) and nuclei were stained for 30 min with 2 µg/ml Hoechst 33342 (Molecular Probes). Excess dye was removed by washing cells 3× with RPMI-A and hematocrit was lowered to 2.5% trough RPMI-A addition. Four volumes of this culture were then added to 1 vol of antibody- or iLP-containing samples to reach, respectively, 70 µg antibody/ml or 1 mM lipid, and 2% hematocrit, and samples were incubated for 1.5 h at 37 °C under orbital mixing. When using the free monoclonal antibody anti-GPA, its concentration was lowered to 1 µg/ml because of excessive RBC agglutination found at higher concentrations, with no significant difference in targeting. iLPs loaded with the fluorescent dye pyranine were observed directly, whereas antibodies were detected with the corresponding fluorescent secondary antibodies as described above, but diluted in RPMI-A. Finally, cells were washed 3× with RPMI-A and placed at 0.2% hematocrit into MatTek culture plates for further analysis with an Olympus IX51 inverted system microscope, equipped with an IX2-SFR X-Y stage, a U-TVIX-2 camera, and a fluorescence mirror unit cassette for UV/blue/green excitation and detection of their respective blue/green/red emission ranges. Phase contrast images were acquired simultaneously.

2.9. Flow cytometry

For growth inhibition determination and quantitative live cell targeting examination of antibodies and iLPs, samples were analyzed at 0.02% hematocrit in PBS with a BD LSRFortessa flow cytometer (Becton, Dickinson and Company, New Jersey, USA). Forward- and side-scatter in a logarithmic scale were used to gate the RBC population. Green fluorescent dyes (Syto11, pyranine, and AF488) and Hoechst 33342 were detected, respectively, by excitation through a 488

or 355 nm laser at 50 mW power and emission collection with a 530/30 or 450/50 nm bandpass filter. Acquisition was configured to stop after recording 20,000 events within the RBC population. Parasitized erythrocytes in late forms were distinguished from those in young forms, when required, by means of their increased DNA and RNA content giving higher Syto11 signal intensity values.

2.10. Transmission electron microscopy (TEM)

P. falciparum cultures sorbitol-synchronized at ring, trophozoite, and schizont stages were washed 3× with PBS (470 *g*, 5 min), and 6-µl volumes of pelleted cells were fixed in 500 µl of 4% v/v formaldehyde in PBS for 1 h at 4 °C under orbital stirring. The fixing solution was changed to 2% v/v formaldehyde in PBS and cells were left in the same solution at 4 °C for 24 h until gelatine embedding. Prior to fixation, ring samples were at 10% parasitemia, whereas trophozoite and schizont stages were enriched to >90% parasitemia in 70% Percoll. After fixation, sample processing for the preparation of ultrathin cryosections was done as previously described [30]. Cryosections were incubated for 30 min in PBS containing 5% fetal bovine serum with the corresponding primary antibodies (mouse *BM1234*, anti-HRP2 and anti-GPA at 40 µg/ml, and rabbit anti-MAHRP1$_{21\text{-}40}$ at 21 µg/ml), followed by secondary antibodies (50 µg/ml goat anti-mouse or goat anti-rabbit IgG H+L) coupled to 12-nm colloidal gold particles (Jackson ImmunoResearch Laboratories Inc., West Grove, PA, USA). As control for non-specific secondary antibody binding the primary antibody was omitted; non-infected red blood cells were also processed as a control for non-specific interactions of the primary antibodies. Sample observations were done in an electron microscope Jeol J1010 (Jeol, Japan) with a CCD SIS Megaview III camera.

For immunocryo-TEM analysis of anti-GPA targeted LPs, a thin aqueous film was formed by dipping a glow discharged holey carbon grid in the LP suspension and then blotting the grid against filter paper. The resulting thin sample films spanning the grid holes were then incubated with a 1:20 v/v dilution of goat anti-mouse IgG (H+L) antibody coupled to 6-nm colloidal gold particles (Jackson ImmunoResearch Laboratories Inc.) for 30 min and washed twice in PBS. Sample vitrification and microscope analysis were done as described previously [10].

2.11. Subcellular protein fractionation

Differential detergent fractionation of pRBC proteins was essentially performed as previously described [31]. PBS supplemented with 1× complete protease inhibitor cocktail (Roche) was used for the washing of cells and as buffer for all detergent-containing samples; all fractions were obtained using the same detergent extraction volume, calculated as 6× pRBC pellet starting volume. Cells were extensively washed and extracted with 0.15% saponin for 10 min at 4 °C, pelleted by centrifugation (10,000 *g*, 15 min, 4 °C), and the resulting supernatant was rescued as the saponin-soluble fraction. The saponin-insoluble pellet was washed again before being extracted with 1% Triton X-100 (30 min, 4 °C). Samples were centrifuged (20,000 *g*, 30 min, 4 °C) and the resulting supernatant was rescued as the Triton-soluble fraction. Finally, the Triton-insoluble pellet was washed again before the final extraction with 2× SDS-containing reducing Laemmli sample buffer (supplemented with 355 mM 2-mercaptoethanol) for 30 min at 60 °C while vigorously mixing by vortex every 10 min. The final SDS-soluble fraction was then collected after spinning down cell debris (16,000 *g*, 15 min). For two-dimensional-PAGE, the Triton-insoluble pellet was extracted with O'Farrell lysis buffer (5% v/v 2-mercaptoethanol, 2% w/v NP-40, 9.5 M urea) [32] for 30 min at 30 °C under sonication (30-second pulses, 100% amplitude) until pellet disgregation. Saponin, Triton, and SDS fractions mainly contained, respectively, cytosolic proteins, membrane and organelle proteins, and nuclear and detergent-resistant cytoskeletal/matrix proteins. Because erythrocytes lack a cell nucleus and have few organelles, most of the proteins from the last two fractions will belong to *P. falciparum*.

2.12. Two-dimensional (2D)-SDS-PAGE

To two 140-µl protein samples (containing 80 µg of total protein each) were added a trace amount of Bromophenol blue and an aliquot of immobilized pH gradient (IPG) buffer to reach a final concentration of 0.5% v/v. For the first dimension isoelectric focusing, samples were loaded onto two 7-cm immobilized pH gradient strips, pH 3-10 (Immobiline® DryStrip, GE Healthcare, Life Sciences), subjected to overnight passive rehydration (13 h, 20 °C) and then run on a IPGphor device (first step-and-hold, 1 h, 50 V; second step-and-hold, 0.5 h, 300 V; third gradient step 0.5 h to reach 1000 V; fourth gradient step, 1.5 h to reach 5000 V; and finally a fifth step-and-hold, 2.5 h, 5000 V; the accumulated voltage was 5632 KV·h). Prior to the second dimension, the IPG strips were equilibrated in two steps for 15 min each with gentle shaking in 3 ml of equilibration buffer (first equilibration solution: 50 mM Tris-HCl, pH 8.8, 6 M urea, 30% w/v glycerol, 2% SDS, 65 mM DTT and a trace amount of Bromophenol blue; for the second equilibration solution, DTT was replaced by 135 mM iodoacetamide). The second dimension SDS-PAGE was performed in a vertical Mini Protean Hoefer system (Hoefer, Inc.). After equilibration, strips were transferred to the second dimension in two 12.5% polyacrylamide gels (0.375 M Tris-HCl, pH 8.8, 0.1% SDS) run for 1 h at 100 V and 20 mA/gel (running buffer: 25 mM Tris-base, 192 mM glycine, 0.1% SDS, pH 8.6). The BenchMark™ Protein Ladder 10747-012 (Invitrogen) was run in parallel as molecular mass marker. One of the gels was silver-stained as described above, scanned (GS 800 Calibrated Densitometer M, Bio-Rad), and the image obtained was processed (Quantity One software image analysis, Bio-Rad). The other gel was transferred to a PVDF membrane (Hybond-P, Amersham Biosciences) and processed for Western blot analysis of proteins as previously described [10]. After incubation with the mouse monoclonal antibody *BM1234* (2 µg/ml) followed by goat anti-mouse IgG horseradish peroxidase-conjugated (1 µg/ml, Thermo Fisher Scientific, Inc.), chemiluminescence was recorded (ImageQuant LAS 4000, GE Healthcare Life Sciences) and the membrane was finally stained with Ponceau S (0.1% w/v in 5% v/v acetic acid) for 10 min. The region containing the two spots detected by *BM1234* was identified by triangulation using protein spots common to Ponceau and silver stains, excised from the silver-stained gel, and subjected to LC-MS/MS for protein identification.

2.13. Liquid chromatography with tandem mass spectrometry (LC-MS/MS)

Trypsin digestion of proteins in silver-stained gel slabs was performed in a ProGest™ automatic digestor (Genomic Solutions). Each sample was washed with 50 mM NH_4HCO_3 and acetonitrile (ACN), reduced in 10 mM DTT (30 min, 56 °C), alkylated in 55 mM iodoacetamide (30 min, 30 °C, protected from light), and digested with 80 ng of porcine trypsin (Trypsin Gold, Promega) for 16 h at 37 °C. The resulting peptides were extracted from the gel matrix with 5% formic acid (FA) and ACN, and dried in a SpeedVac concentrator. LC-MS/MS identification was performed in a Cap-LC-nano-ESI-Q-TOF system (Micromass-Waters). Dried peptides were taken up in 100 µl of 1% FA and 4-10 µl of the resulting solution was injected into the liquid chromatography system equipped with a reverse phase C18 column (75 µm internal diameter, 3 µm particle, 15 cm length; NanoEase Atlantis, Waters), with a mobile phase gradient 5-60% B in 35 min (A: 2% ACN, 0.1% FA; B: 90% ACN, 0.1% FA). Eluted peptides were ionized trough electrospray (NanoES PicoTip™ emitter, New Objective) with an applied voltage of 2 KV to capillary/needle and 60 V to cone. A 400-1,800 m/z range of peptide masses was analyzed in full scan MS mode (1 s scan time, 10,000 full width at half maximum resolution). Within this range, the 10 most abundant peptides were selected (minimum intensity of 28 counts/second) for their fragmentation by collision-induced dissociation (20 eV collision energy, Ar gas) in the MS/MS analysis (1 s scan time, 100-1,700 m/z range). Peptide fragmentation generated a pkl file (MassLynx MS software) and sequences were matched with the NCBInr on-line database using the MASCOT search engine.

2.14. Determination of LP half-life time in blood plasma

LPs fluorescently labeled and PEG-grafted (DOPC:cholesterol:DOPE-Rho:PE-PEG2000, 64:20:1:15), were injected intravenously at 200 mg/kg doses to ICR-CD1 mice females of ca. 23 g (Harlan Laboratories). Blood samples of ca. 30-40 µl were then collected in Microvette heparinized tubes (Sarstedt) from the terminal portion of the tail at the post-administration times: t_0 (2 min), 1.5 h, 6 h, 24 h, 48 h and 72 h. Samples were separated into supernatant (plasma, stored at −80 °C until analysis) and cells by centrifugation at 4,000 *g* for 3 min. For fluorescence quantification of LPs containing the rhodamine-conjugated lipid DOPE-Rho, plasma samples were thawed on ice, diluted with one volume of 2% Triton X-100 in PBS and 5 replicas of 2-µl drops were placed on a methanol-activated PVDF membrane. Fluorescence signal from spotted samples was imaged and analyzed with an ImageQuant LAS 4000 biomolecular imager with green RGB light source and 1/100- to 30-s exposure time. Plasma autofluorescence signal was subtracted from samples using plasma collected from an untreated mouse. LP concentration was calculated by linear regression using serial-fold dilutions of stock LPs in PBS spotted on the same membrane at known concentrations. Finally, concentration values were normalized to t_0 (100%) and LP half-life time ($t_{1/2}$, time after which 50% of the administered LPs are removed from plasma), was determined.

2.15. In vivo 4-day test in P. falciparum-infected mice

Female immunodeficient NOD.Cg-*Prkdc*^{scid} *Il2rg*^{tm1Wjl}/SzJ (NOD scid gamma, NSG) mice were engrafted with human erythrocytes and infected i.v. with the *P. falciparum* 3D7$^{0087/N9}$ strain generated in GlaxoSmithKline (Tres Cantos, Spain), using established methods [33]. These mice sustain in circulation high amounts of human RBCs (ca. 1 to 1.75×10^{10} in 2.5 ml blood). The inoculum was 2×10^7 *P. falciparum*-infected erythrocytes, and free or encapsulated drugs were administered i.v. in PBS for four consecutive days starting at day 3 after infection, using 2 mice/compound. Parasitemia was measured by flow cytometry as described [34], with 0.01% sensitivity of detection. Sampling was every 24 hours after start of treatment until end of assays. Effective dose 50% (ED_{50}) and ED_{90} are defined as the dose in mg/kg that reduces parasitemia at day 7 after infection by 50% and 90%, respectively, relative to vehicle-treated mice. The human biological samples were sourced ethically and their research use was in accord with the terms of the informed consents. All animal studies were ethically reviewed and carried out in accordance with European Directive 86/609/EEC and the GSK Policy on the Care, Welfare and Treatment of Animals.

3. Results

3.1. Passive vs. active encapsulation methods for the entrapment of antimalarial drugs into LPs

Because of their amphiphilic nature, depending on pH the weak basic antimalarial drugs chloroquine (CQ) and primaquine (PQ) are found in their uncharged, monoprotonated and diprotonated forms (Fig. 2), which have different organic/aqueous partitioning degrees. The encapsulation efficiencies (EEs) of CQ and PQ passively loaded through the lipid film hydration method [20] into LPs composed mainly of neutrally charged unsaturated phospholipids (DOPC:cholesterol, 80:20) were determined at different lipid film hydration solution pHs and initial drug concentrations (Table 1). Passive EE was several-fold higher for PQ vs. CQ, which can be explained because of their different protonation degree. Whereas for the wide pH range 4.0-7.4 CQ becomes fully protonated (≥99% CQ^{2H+}), PQ is found mainly in its monoprotonated species (≥86% PQ^{H+}), which confers PQ a lower ionization state and therefore higher hydrophobicity and interaction with the LP lipid bilayer. The significant EE increase for lower drug amounts at a fixed pH (Supplementary Table 1) indicates saturation of passive LP encapsulation capacity. On the other hand, in agreement with previous reports [21,35,36], active encapsulation of CQ and PQ by

establishing a pH gradient 4.0-7.5 inside-outside of LPs composed mainly of neutrally charged saturated phospholipids (DSPC:cholesterol, 90:10) resulted in EE values close to 100% (Table 1). Drug amounts during active encapsulation into LPs were selected according to the aforementioned works as those highest possible while avoiding a significant consumption of the internal liposomal proton pool.

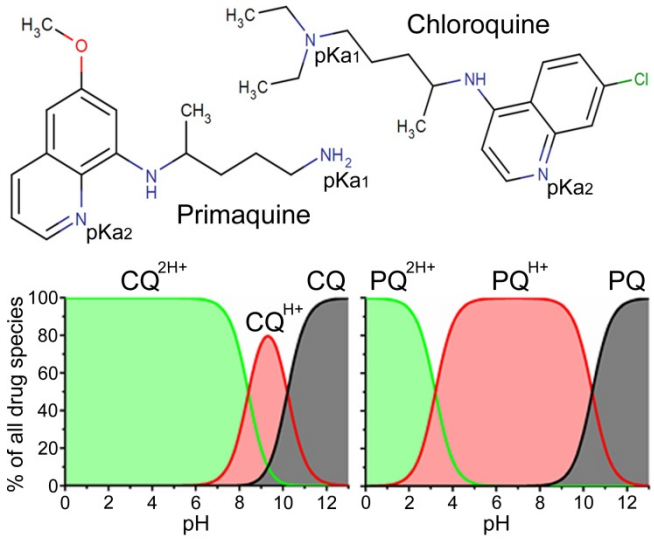

Fig. 2. Ionization species in solution as a function of pH for the weak basic drugs chloroquine (CQ, pKas 10.2 and 8.4 [37]) and primaquine (PQ, pKas 10.4 and 3.2 [38]). Chemical formulae were obtained from http://www.chemicalize.org/.

Table 1. Passive (DOPC LPs) and active (***DSPC LPs***) encapsulation efficiencies (EE) for CQ and PQ into LPs at 10 mM total lipid.

Liposomal samples	Added drug (μM)	Encapsulated drug (μM)	EE (%)
DOPC CQ pH 7.4	10000	999.0 ± 5.2	10.0 ± 0.1
DOPC CQ pH 6.5	10000	499.0 ± 12.1	5.0 ± 0.1
DOPC CQ pH 6.5	25	3.5 ± 0.6	14.1 ± 2.5
DSPC CQ pH 4.0 - 7.5	***500***	***491.7 ± 1.6***	***98.3 ± 0.3***
DOPC PQ pH 7.4	10000	3392.6 ± 70.9	33.9 ± 0.7
DOPC PQ pH 6.5	10000	3215.0 ± 61.9	32.2 ± 0.6
DOPC PQ pH 6.5	4000	1945.9 ± 78.0	48.7 ± 2.0
DSPC PQ pH 4.0 - 7.5	***1000***	***966.7 ± 2.1***	***96.7 ± 0.2***

After 2 weeks in storage conditions (PBS, pH 7.4, 4 °C) insignificant release (<5 %) was obtained for actively encapsulated drugs (Fig. 3A). By contrast, drugs were quickly released when passively encapsulated, with ca. 60% and 30% of originally encapsulated CQ and PQ, respectively, being found outside LPs after only 5 min storage. In accordance with passive encapsulation data for DOPC LPs (Table 1), PQ was significantly more retained than CQ (Supplementary Table 2), with respective encapsulated amounts at equilibrium of ca. 60% and 20%. Similar drug release results were obtained in *P. falciparum* culture conditions (PBS, pH 7.4, 37 °C, diluted samples; Fig. 3B). Whereas passively encapsulated CQ was almost completely released after 48 h under culture conditions, 30% of PQ was still retained in LPs, reflecting the higher hydrophobicity of PQ and its stronger lipid bilayer interaction. On the other hand, no significant release of actively encapsulated drug was observed under the same experimental conditions during the first 3 h of incubation, illustrating the capacity of the pH gradient method for amphiphilic drug containment into LPs.

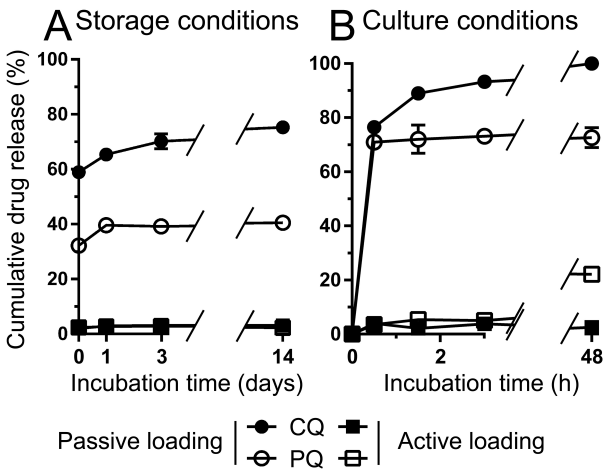

Fig. 3. Cumulative drug release of encapsulated CQ and PQ passively loaded (DOPC liposome, 10 mM drug during encapsulation) and actively loaded (DSPC liposome, drug concentrations in Table 1) under (A) storage conditions (4 °C, 10 mM total lipid) and (B) culture conditions (liposomal samples in storage conditions further diluted 1:10 and 1:40 in PBS for CQ and PQ, respectively, and incubated at 37 °C).

3.2. Targeting antibodies against different pRBC antigens

A previous iLP prototype developed in our group was able to improve ca. 10-fold the efficacy of CQ *in vitro* [10], although most of this effect was due to liposomization of the drug, and only a relatively minor effect could be attributed to antibody (Ab) targeting [12]. Since the antigen of the pRBC-binding *BM1234* commercial monoclonal antibody used was not known, we set out to identify it. The *BM1234*-positive, Triton X-100-insoluble fraction of a pRBC extract (Fig. S1) was analyzed in a 2D-PAGE/Western blot and the area containing the two spots detected by *BM1234* (Fig. S2A) was excised from an identical 2D-PAGE run in parallel (Fig. S2C) and subjected to LC-MS/MS analysis (data not shown). The resulting peptides indicated that the *BM1234* antigen was the membrane-associated histidine-rich protein 1 (MAHRP1), found in two major isoforms as previously described [39]. Subcellular fractionation analysis along the intraerythrocytic *P. falciparum* cycle (Fig. S3) confirmed the presence of the antigen mostly within insoluble membrane fractions of the late stages trophozoites and schizonts, in agreement with the expected preferential localization of the protein in Maurer's clefts [40], organelles involved in trafficking of several proteins towards the pRBC membrane [16,41]. Despite the intracellular location of MAHRP1, the improved pRBC targeting of *BM1234* iLPs over LPs [10] suggested that at some time the recognized antigen should be exposed on the pRBC membrane. Indeed, MAHRP1 had been described as being essential for the translocation to the pRBC surface of PfEMP1, a mediator of pRBC cytoadherence to cell membrane receptors [42]. The association between these two proteins in pRBC plasma membrane regions has been confirmed by confocal fluorescence microscopy (Fig. S4). Consistent with these observations, TEM data showed the expected preferential intracellular localization of the *BM1234* antigen, but with some occasional host cell plasma membrane-associated signal (Fig. S5). Since MAHRP1 was suggested to bind erythrocytes through a 20-mer-long amino acid region [43], we decided to generate polyclonal antibodies against this peptide (ADVPTEGMDVPFGFFDKNTL). As expected, the antigen detected by the resulting antibodies, $MAHRP1_{21\text{-}40}$, showed a subcellular localization similar to that of the BM1234 antigen (Figs. S6 and S7).

Knowing the preferential intracellular localization of MAHRP1, we explored other protein targets present on pRBC surfaces for which commercial antibodies were available: Histidine-rich protein 2 (HRP2) [44] and glycophorin A (GPA) [45]. HRP2 is expressed during most of the *P. falciparum* life cycle (Fig. S3) and secreted by pRBCs, being therefore at some point present on the extracellular side of the plasma membrane (Figs. S8 and S9). GPA is a conserved and highly

abundant membrane protein present in all RBCs and pRBCs (Fig. 4A). To test the targeting capacity of the selected antibodies, these were incubated with live pRBC cultures and analyzed directly without fixation by flow cytometry (Fig. 4B) and by fluorescence microscopy (Figs. 4C and S10). In these conditions, anti-GPA proved to be the only antibody capable of completely recognizing the entire RBC and pRBC populations, whereas *BM1234*, anti-HRP2, and anti-MAHRP1$_{21\text{-}40}$ bound just a small fraction of pRBCs (<1%), in agreement with the different extracellular exposures of the respective antigens.

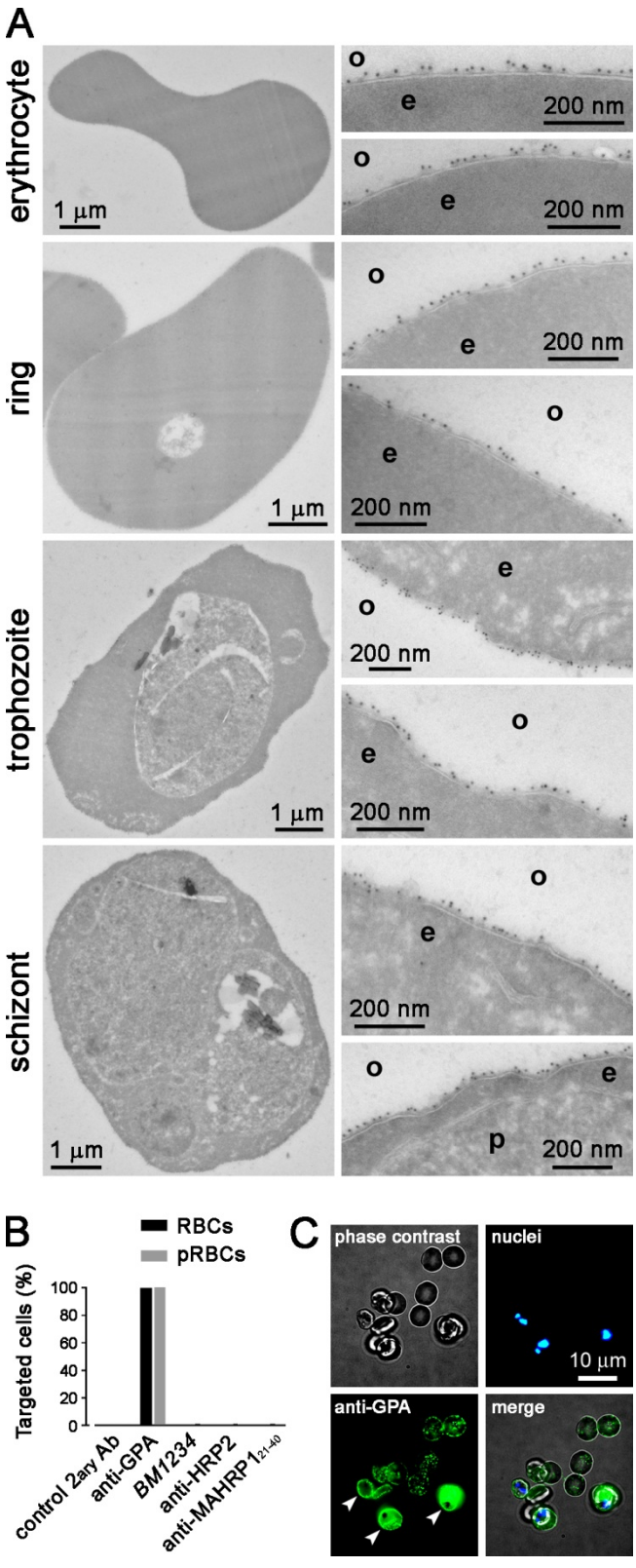

Fig. 4. Cell targeting analysis of monoclonal anti-GPA antibody. (A) Immuno-TEM subcellular localization analysis in RBCs and in pRBCs at the ring, trophozoite, and schizont stages of erythrocytic glycophorin A. o: outside of the cell; e: erythrocyte cytoplasm; p: *P. falciparum*. (B) Flow cytometry analysis of the binding of targeting antibodies to non-fixed RBCs and pRBCs. (C) Epifluorescence microscopic analysis of the binding of anti-GPA to live RBCs and pRBCs. Arrowheads indicate the three pRBCs present in the image.

3.3. Binding of targeting antibodies to LPs

The capacity of the antibodies raised against MAHRP1 (*BM1234* and anti-MAHRP1$_{21\text{-}40}$), HRP2, and GPA as targeting agents for the functionalization of iLPs (DOPC:cholesterol:MPB-PE, 65:20:15) was tested *in vitro* with live cells by fluorescence microscopy. iLPs containing in their formulation 0.5% of the rhodamine-labeled lipid DOPE-Rho, and loaded with 30 mM pyranine for tracking purposes, were subsequently functionalized with free thiol-bearing half-antibodies by crosslinking these to lipids containing thiol-reacting maleimide (Mal) groups as previously described [10] (Fig. S11). Consistently with the results obtained using free antibodies, of the four LP-Mal-antibody (LP-Mal-Ab), only anti-GPA iLPs were capable of completely recognizing target cells in live pRBC cultures (Fig. S12), though only at the high LP concentration of 1 mM total lipid. In an attempt to improve anti-GPA-iLP targeting, three alternative iLP models were designed (Fig. 5). A lipid bearing a 2-kDa polyethylene glycol (PEG) linker terminated with a Mal group (DSPE-PEG-Mal) was included in the LP formulation (5% of total lipid; LP-PEG-Mal) with the double objective of (i) providing better antigen access to targeting Abs and (ii) improving the coupling reaction otherwise sterically hindered in the original iLP model by the polar heads of surrounding lipids [46,47]. This strategy was used for the oriented binding of half-antibodies through their free thiols (LP-PEG-Mal-Ab) or of whole antibodies through the carbohydrate moieties in antibody Fc regions (LP-PEG-Mal-CHO-Ab), and for the non-oriented binding through primary amino groups on Ab amino acid residues (LP-PEG-Mal-NH_2-Ab). To support a pH gradient required for the active encapsulation of amphiphilic drugs, the LP formulation was adapted by including the saturated lipid DSPC and lowering the cholesterol content. The relative amounts of Mal-conjugated lipid and antibody were adjusted to a lipid:Ab 75-fold molar excess during coupling to maximize binding yield, with a final lipid composition DSPC:cholesterol:DSPE-PEG-Mal 85:10:5. Analysis of anti-GPA iLPs showed that all four methods resulted in good coupling efficiencies above 30% of total antibody added (≥55 Ab molecules/LP), with LP-PEG-Mal-NH_2-Ab showing the best results (Fig. 6 and Table 2). Protein smears observed in the gel lanes corresponding to samples coupled through primary amines indicate an efficient incorporation of maleimide-containing lipids and SATA crosslinker molecules, which decreased the electrophoretic mobility of antibody chains.

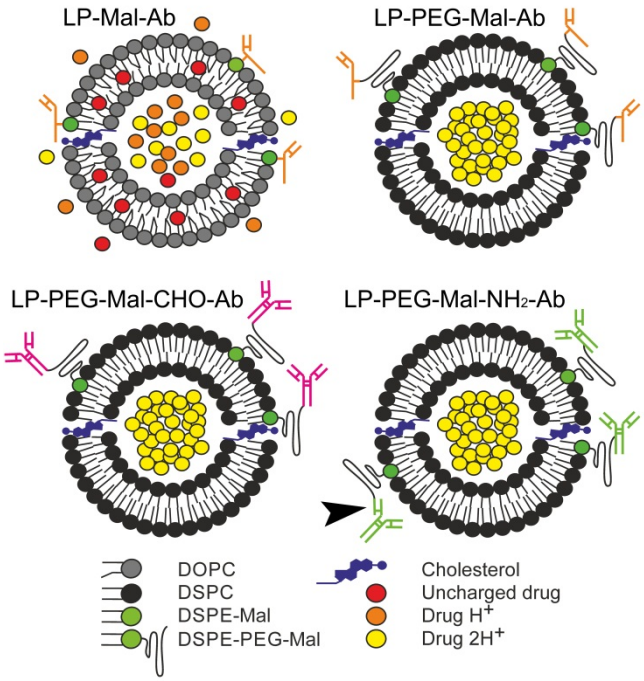

Fig. 5. Representation of iLP models encapsulating an amphiphilic weak basic drug and functionalized with antibodies linked through four different conjugation strategies, all based on the formation of a thioether bond between a thiolated antibody and a maleimide-conjugated lipid. For cell targeting assays, drugs were substituted by the fluorescent dye pyranine as a tracker for the LP aqueous core and a rhodamine-conjugated lipid (DOPE-Rho) was included in the LP formulation. LP-Mal-Ab and LP-PEG-Mal-Ab: half-antibody is conjugated in oriented position, in the second model at the distal end of a 2-kDa PEG linker. LP-PEG-Mal-CHO-Ab: whole antibodies are conjugated in oriented position through the carbohydrate chains in the Fc region. LP-PEG-Mal-NH_2-Ab: whole antibodies are conjugated in non-oriented position through primary amino groups, which in some cases can be placed within the antigen binding site, interfering with antigen recognition (arrowhead). In the first model the drug is represented as being passively loaded, whereas the other three models represent drug actively loaded with the pH gradient method.

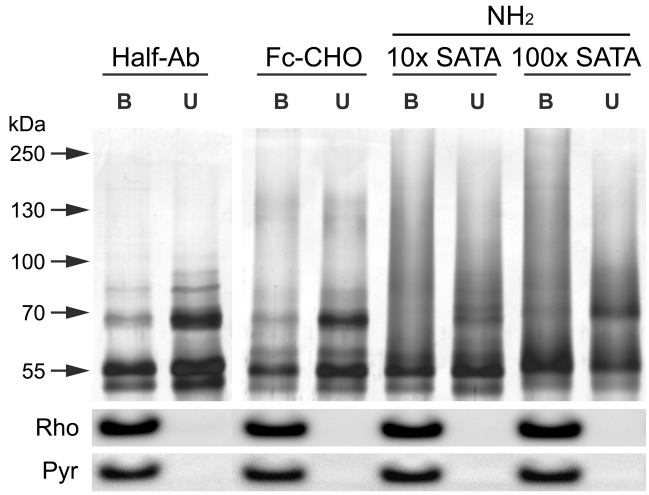

Fig. 6. Silver-stained, reducing SDS-PAGE analysis of different strategies for the coupling of anti-GPA polyclonal antibodies to LPs. Coupling was via a PEG-Mal linker through: (Half-Ab) the free thiol of half-antibodies, LP-PEG-Mal-Ab model; (Fc-CHO) the carbohydrate moiety in Fc regions, LP-PEG-Mal-CHO-Ab model; (NH_2) primary amino groups with different amounts of the crosslinking agent SATA (10× and 100× molar excess relative to antibody molecules), LP-PEG-Mal-NH_2-Ab model. Prior to electrophoresis, samples containing 2 µg protein were centrifuged for the analysis of LP-bound antibodies in the pellet (B) and of unbound antibodies in the supernatant (U). The ca. 70-kDa band with a relatively minor incorporation

into LPs when compared to the ca. 55-kDa band of IgG heavy chains, corresponds to rabbit albumin, which is highly abundant in animal serum and interacts with Protein G during IgG purification [48]. When using monoclonal antibodies, albumin is absent (Fig. S13). The fluorescence emission of rhodamine (Rho) conjugated to lipids included in the formulation of LPs, and of pyranine dye (Pyr) with which they were passively loaded, are used as controls of the LP-containing fractions.

Table 2. Characterization of the different methods used to conjugate the polyclonal anti-GPA antibody to maleimide-PEG-grafted LPs (LP-PEG-Mal model).

Parameter	Half-Ab	Fc-CHO	NH_2 10× SATA	NH_2 100× SATA
Sulfhydryl groups / Ab	0.7 ± 0.4	1.9 ± 0.5	2.9 ± 0.4	10.2 ± 0.1
Coupling efficiency (%)	32.5 ± 5.0	39.6 ± 2.2	44.1 ± 1.5	54.4 ± 0.0
µg Ab / µmol lipid	34.6 ± 5.3	32.1 ± 1.8	53.3 ± 1.8	67.1 ± 0.0
Ab number per LP	55.6 ± 8.5	51.6 ± 2.8	85.6 ± 2.8	107.6 ± 0.0
Size increment (nm)	4.9 ± 3.4	0.0 ± 4.4	8.7 ± 3.3	17.1 ± 1.3

3.4. Cell targeting of iLPs

Flow cytometry studies on non-fixed RBCs using the different iLP models indicated a cell targeting efficiency LP-PEG-Mal-NH_2-Ab >> LP-PEG-Mal-CHO-Ab >> LP-Mal-Ab/LP-PEG-Mal-Ab (Fig. 7A). After a 30-min incubation, only ca. 10% of cells were bound by LP-Mal-Ab anti-GPA iLPs at 250 µM lipid in culture, whereas LP-PEG-Mal-NH_2-Ab generated using the relatively low crosslinker:Ab 10× molar excess resulted in ~100% cell targeting at a concentration of 100 µM lipid. This complete targeting could be maintained when using a monoclonal anti-GPA (LP-PEG-Mal-NH_2-MAb-10×) even at a LP concentration of 50 µM lipid, and down to 0.5 µM lipid according to fluorescence microscopy analysis (Fig. S14). Cryo-TEM images showed that >90% of LPs in this last model carried antibodies (Fig. S15), result consistent with the observation that >80% of LPs are retained on target cells at ≤50 µM lipid, whereas retention values were below 15% for all other iLP models (Fig. 7B). It is important to note that using a 10-fold increase of the chemical crosslinker SATA (100× molar excess) inhibited cell targeting (Fig. 7), likely due to massive crosslinking of NH_2 groups near the antigen recognition site of antibodies. When LP-PEG-Mal-NH_2-MAb-10× iLPs were incubated with live pRBC cultures for 90 min, confocal fluorescence microscopy analysis showed colocalization of rhodamine and pyranine signals on RBCs and pRBCs as a punctate pattern (Fig. 8A-C). This suggested that erythrocyte-bound iLPs did not immediately fuse with the plasma membrane, but rather remained adsorbed onto the cell. The observation of the presence of diffuse fluorescence areas in some RBCs (Fig. 8B), but especially on pRBCs (Fig. 8C), suggests that eventually iLPs could fuse with the cell, despite the lipid formulation used here (dominated by saturated lipids) significantly inhibits such fusion events. Free pyranine controls showed passive entry of this highly hydrophilic dye only into pRBCs (Fig. 8D).

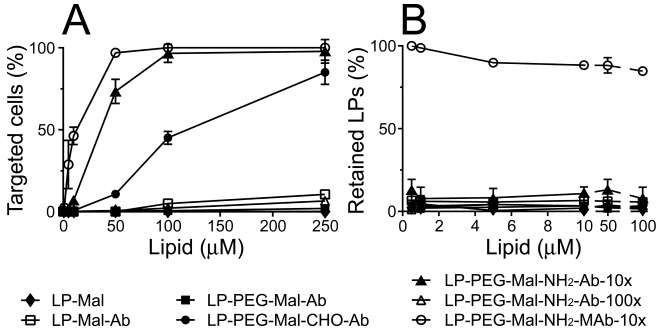

Fig. 7. RBC targeting analysis after a 30-min incubation with anti-GPA iLPs loaded with 30 mM pyranine and prepared through different antibody conjugation methods. (A) Flow cytometry results showing the fraction of RBCs positive for pyranine signal. (B) Determination by pyranine fluorescence quantification in

the culture supernatant of the iLP fraction bound to cells. All samples were prepared with polyclonal antibodies except LP-PEG-Mal-NH_2-MAb-10×, where a monoclonal antibody was used.

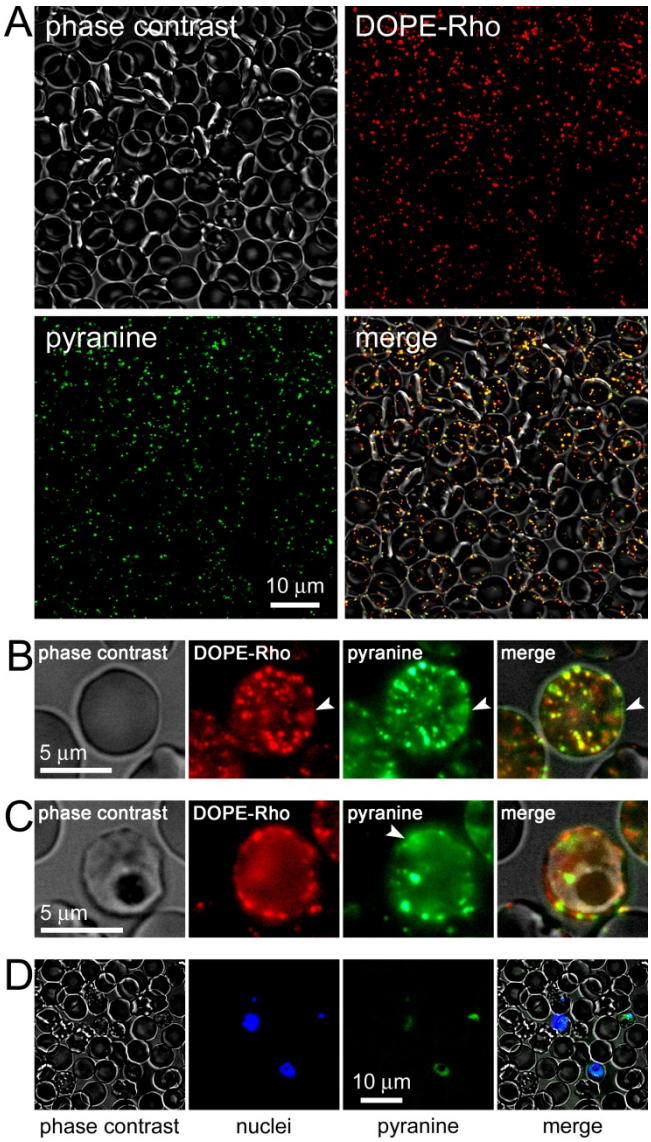

Fig. 8. Fluorescence microscopy analysis of the interaction of anti-GPA iLPs with target cells. Rhodamine-labeled anti-GPA LP-PEG-Mal-NH_2-Ab iLPs loaded with pyranine (concentrations in the culture of 500 µM lipid and 26 µM pyranine) were added to live pRBC cultures, incubated for 90 min and visualized without fixation by (A) confocal fluorescence microscopy and (B, RBC; C, pRBC) epifluorescence microscopy. The arrowheads indicate diffuse fluorescence areas. (D) Control sample where 26 µM free pyranine was added to the culture.

3.5. P. falciparum growth inhibition activity of anti-GPA iLPs encapsulating antimalarial drugs

The iLP prototype having both best targeting efficiency and retention into pRBC cultures (LP-PEG-Mal-NH_2-MAb-10× functionalized with monoclonal antibodies against human GPA) was selected for *in vitro* growth inhibition assays of *P. falciparum*. Drug concentrations during active encapsulation of 500 µM CQ and 1 mM PQ (for 10 mM total lipid) were selected to avoid an excessive consumption of the LP internal proton pool and subsequent disruption of the liposomal pH gradient [21,35], yielding EEs of 98.3 and 96.7% for CQ and PQ, respectively (Table 1). After only 15 min of incubation in the presence of iLPs, pRBC cultures were washed and incubated for a further 48 h (one replication cycle). CQ activity significantly improved when actively encapsulated

into iLPs, with an IC50 of ca. 35 nM when administered to *P. falciparum* cultures synchronized in either ring or late blood stages (trophozoites + schizonts), whereas at a concentration of 50 nM encapsulated CQ, parasite growth was completely inhibited (Fig. 9A,B). In contrast, free CQ was only capable of completely inhibiting *Plasmodium* growth when added to late forms at a concentration in culture of 200 nM, although this dose was ineffective when added to ring stages. Neither agglutination nor morphological alterations of RBCs were observed upon microscopic examination of Giemsa-stained slides from growth inhibition assays (Fig. S16). Fluorescence microscopy and flow cytometry analysis (Fig. S17), as well as hemolysis assays (Fig. S18), further confirmed an absence of adverse effects on non-infected RBCs within the liposome molar range leading to complete *P. falciparum* growth inhibition (1-4 μM lipid, corresponding respectively to ca. 19-75 iLPs/RBC; Fig. S19), indicating that erythrocyte viability was not compromised by iLP binding. When ≥50 nM CQ encapsulated in iLPs was added at ring stage, the parasites were killed before completing their intraerythrocytic cycle, as evidenced by a lack of increase in pRBC numbers after 48 h and the microscopic observation of picnotic *Plasmodium* nuclei indicative of cell death (Fig. S16A). On the other hand, when added to late stages, treated parasites egressed from pRBCs but had a low invasion rate and those which could invade RBCs failed to mature into late forms, dying at ring stage. Again, this growth inhibitory effect was evidenced by pRBC counts and microscopic examination (Fig. S16B). Fluorescence microscopy detection at the end of growth inhibition assays of DOPE-Rho lipid that had been incorporated into the LP formulation confirmed the expected iLP binding to all RBCs and pRBCs (Fig. S20). In late forms, lipid fluorescence was often observed to be homogeneously distributed throughout the cell, hinting at LP fusion with the pRBC membrane during the length of 48-h growth inhibition assays. Dramatic activity increases were also obtained for actively encapsulated PQ, which at 10 μM eliminated parasitemia almost completely in both ring and late form cultures, whereas the same concentration of free drug did not have any significant effect on the parasite (Fig. 9C). However, PQ-containing iLPs had *in vitro* an RBC agglutinating effect (Fig. 9D-F), likely due to the need to add a large amount of drug-encapsulating LPs (50-100 μM lipid, corresponding respectively to 940-1,880 iLPs/RBC; Fig. S19) because of the high *in vitro* IC50 of PQ, which is in the μM range. This agglutinating effect was especially significant under static incubation conditions for high iLP amounts >10 μM lipid (Figs. S17 and S19). Absence of hemolysis was observed even for the highest agglutinating iLP amount of 100 μM lipid (Fig. S18).

Preliminary *in vivo* 4-day tests in mice grafted with human erythrocytes and subsequently infected with *P. falciparum* showed that anti-GPA iLPs (LP-PEG-Mal-NH_2-MAb-10×) encapsulating CQ cleared the pathogen below detectable levels (<0.01% parasitemia in peripheral blood) at a CQ dose of 0.5 mg/kg, whereas free CQ administered at 1.75 mg/kg was, at most, 40-fold less efficient (ca. 0.4% parasitemia; Fig. 10). 0.5 mg CQ/kg administered in non-targeted liposomes had a much diminished effect, which highlights the crucial role of GPA targeting. The survival of iLP-treated mice suggests that the function of non-infected RBCs was not significantly affected *in vivo* by CQ-loaded iLPs at the concentration required to eliminate parasitemia from infected animals.

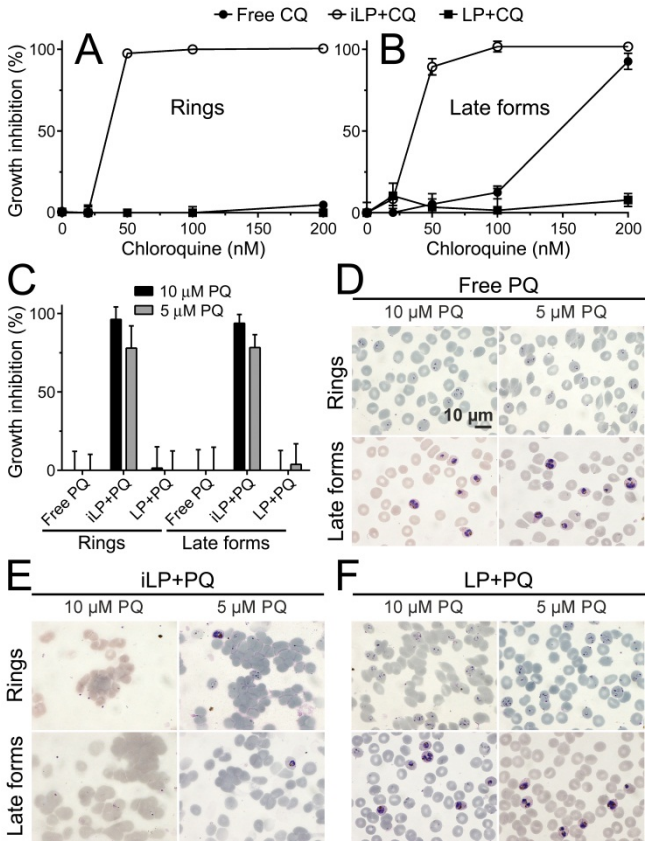

Fig. 9. *P. falciparum* growth inhibition assays of the effect of CQ and PQ as free drugs and encapsulated in LPs and iLPs. CQ (A, B) and PQ (C) encapsulated in LP-PEG-Mal-NH_2-Mab anti-GPA iLPs, in LP-PEG-Mal LPs, or in non-encapsulated form were added at the same final concentrations to either ring or late blood stages (trophozoites and schizonts) and let to act for 15 min before removing them by changing the incubation medium. After a further 48 h incubation the samples were analysed by flow cytometry to determine *P. falciparum* growth. For PQ samples are shown images of cultures treated with free PQ (D), iLP-PQ (E), and LP-PQ (F), to show agglutination in the iLP-treated samples. Highest LP concentrations in *P. falciparum* cultures were 100 µM and 4 µM lipid for 10 µM PQ and 200 nM CQ, respectively.

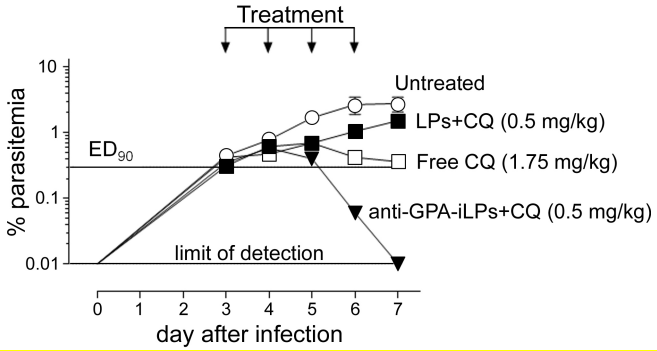

Fig. 10. 4-day test in female immunodeficient mice engrafted with human RBCs and infected i.v. with *P. falciparum*. The animals were treated with the indicated drug preparations at days 3 to 6 after infection. The anti-GPA-iLP+CQ sample contained 48 mmol CQ/mol lipid, whose administered dose corresponded to ca. 100 iLP/erythrocyte, assuming 1×10^{10} human RBCs in the mouse blood circulation.

4. Discussion

Plasmodium early stages are ideal therapeutic targets because drugs delivered to them would have a longer time to kill the parasite before it completes its development, although the permeability of the infected erythrocyte to ions and small nonelectrolytes, including some drugs, does not increase until ca. six hours after invasion [17]. During its maturation the parasite hydrolyzes

hemoglobin in a digestive vacuole, which is the target of many amphiphilic drugs that freely cross the RBC membrane and accumulate intracellularly. As a result, most antimalarials start affecting the infected cell relatively late in the intraerythrocytic parasite life cycle, when their effect is probably often too short to be lethal for *Plasmodium*.

A strategy to improve the activity of antimalarial drugs contemplates their encapsulation in nanocarriers specifically targeted to pRBCs [49], which requires the existence of specific pRBC markers. 200-nm LPs studded with heparin or specific antibodies raised against pRBCs have been shown to bind late stages with high specificity [10,50], increasing up to tenfold the efficacy of encapsulated antimalarial drugs *in vitro* [12,50]. However, the therapeutic administration of such liposomal models against late stages has to be timed to the precise moment when trophozoites and schizonts are present in blood, between 24 and 48 h into the *P. falciparum* intraerythrocytic cycle. The relatively short blood half-life of, in the best case, <10 h for polyethylene glycol-coated stealth LPs [51], guarantees that if injected when early stage pRBCs are present, by the time late forms mature most LPs will have been removed from the blood circulation. Polymeric nanovectors were observed to penetrate trophozoites and schizonts [30], most likely through the TVN, although entry of nanoparticles into early ring stages has not been observed so far for *P. falciparum* or any other human malaria species. As an additional obstacle to antimalarial targeted delivery strategies, most externally recognizable pRBC proteins are present in the parasite genome as multiple variants that can be clonally expressed [15]. *In vitro*, the targeting of pRBCs using laboratory strains of *Plasmodium* that present known, homogeneously expressed antigens is a valid approach allowing for the use of the corresponding antibody specific for each particular target molecule, but in a clinical setting this strategy is invalidated by the large clonal variability inherent to a typical malaria infection.

Malaria is a systemic infection of erythrocytes, where targeted drug delivery approaches are complicated by the fluidics conditions found in the blood circulation, whose strong flow drag and shear forces necessarily affect the interaction of molecular components with target cells. In this adverse physical environment, the design of iLPs engineered to encapsulate antimalarial drugs for their specific entry into pRBCs has to be especially careful regarding the liposomal nanocapsule composition, which will define drug encapsulation and partition within the vesicle, and the selection of targeting antibody/antigen pairs. Although the oriented binding of half-antibodies through their free thiols or of whole antibodies through their carbohydrate moieties in the Fc region is *a priori* a guarantee to increase antigen binding site exposure and thus target binding efficiency, our results indicate that non-oriented binding through primary amino groups significantly increases the number of antibodies bound per LP, whereas carefully choosing the amount of chemical crosslinker used preserves a high antigen binding capacity, at least for the monoclonal anti-GPA antibody used here. Considering the limitations exposed above for an efficient pRBC targeting, efforts have to be invested in encapsulating the highest drug cargo possible. Using the pH gradient active loading method [36] and LP formulations high in saturated lipids capable of sustaining a proton gradient, we have obtained for the weak basic drugs CQ and PQ encapsulation efficiencies close to 100% and high intraliposomal retention levels >95% for several hours in both storage and culture conditions. However, the varied physicochemical properties of present and future antimalarial drugs will determine their location within the liposomal structure [52,53], calling for encapsulation strategies adapted to each particular compound.

Antimalarial drug carriers should provide optimal drug half-lives in circulation, adequate clearance mechanisms, restriction of unintended drug effects in non-target cells, specific delivery to the correct tissue, and a timely initiation and termination of the therapeutic action. Considering the interest in targeting intraerythrocytic *Plasmodium* as early in its life cycle as possible and the lack of strategies to shuttle drugs into it, alternative approaches must be explored without preconceptions. A way to overcome the aforementioned exposed obstacles to the design of pRBC-targeted nanocarriers can perhaps be provided by one of the most adequate vascular carriers ever proposed; namely, red blood cells themselves [54]. Human erythrocytes have a life span in the blood of up to 120 days, which makes them attractive carriers for intravascular delivery because

they prolong drug circulation. In addition, their large size (ca. 7 μm across and around 2 μm thick) significantly restricts unintended extravasation and in principle allows for a much larger encapsulation capacity than LPs. Other interesting features of RBCs as drug carriers are their biocompatibility and the existence of natural mechanisms for their safe elimination from the body. Actually, delivery of antimalarials to non-infected red blood cells to study the effects on later invading parasites has been an approach used for chemotherapeutic investigations, where pretreatment of erythrocytes with the drugs halofantrine, lumefantrine, piperaquine, amodiaquine, and mefloquine showed that these diffuse into and remain within the cell, inhibiting downstream growth of *Plasmodium* [55]. Nevertheless, the loading of drugs into non-infected RBCs has not yet been explored in detail as a clinically feasible therapeutic strategy against malaria, since most currently available protocols use a harsh *ex vivo* erythrocyte isolation followed by drug loading through diffusion [54].

RBC-targeted iLPs could be used to shuttle into the cell antimalarial drugs, although the incapacity of mature erythrocytes to endocyte [56] calls for the development of specific targeted delivery strategies independent from the receptor-mediated endocytic pathway. Delivery of iLP cargo into RBCs had been proposed to occur through membrane fusion [7], a highly controlled process that requires the incorporation of specific fusogenic agents into the lipid bilayer [57,58]. Nevertheless, because of little evidence for liposomal fusion observed with RBCs, alternative routes for the incorporation of LP contents into targeted erythrocytes should be examined [53]. The TVN induced by *Plasmodium* during its intraerythrocytic growth [17] extends from the parasitophorous vacuole membrane and connects the intracellular parasite with the host RBC surface. However, this confers to the pRBC the capacity of internalizing a wide range of particles up to diameters of only 70 nm [17,59], well below the mean size of the LPs used here. Other potential mechanisms to consider include LP adsorption on the cell surface followed by either the exchange of hydrophobic molecules (e.g. the antimalarial drugs lumefantrine and halofantrine) between apposed lipid bilayers [60,61], or a sustained release of the entrapped material [53]. This process would be mediated by a depletion of the liposomal proton gradient by means of temperature, LP-cell interaction events [62] and lipid sequestration by plasma components [63], and might be highly effective for the delivery of weak basic drugs such as those from the aminoquinoline family. These compounds, positively charged at acidic/neutral pH, will theoretically accumulate inside the cell by virtue of the electrochemical gradient created by the phospholipid asymmetry in RBC membranes [64], which maintains a negatively charged intracellular membrane lining. Although the slow drug release observed for pH gradient-loaded LPs is a requirement for storage periods and to avoid drug leaking before reaching their target, once docked to pRBCs liposomal contents must enter the cell. Here, we have observed for CQ a similar *in vitro* IC50 when present either for 48 h as free drug or for only 15 min encapsulated in iLPs, suggesting an adequate drug transfer from iLP to cell.

Other foreseeable limitations to targeting RBCs as an antimalarial strategy will have to be considered. First, to avoid erythrocyte agglutination, an upper iLP concentration threshold must be established *in vivo*, which will complicate the application of this model to drugs with a high IC50. In this regard, according to the data reported here for drugs having a low IC50 like CQ, a ratio of ca. 100 iLP/RBC (lacking agglutination and hemolysis activity *in vitro*) led in mice grafted with human erythrocytes to complete elimination of parasitemia. A second requirement for the use of RBCs as antimalarial carriers is that when present at therapeutically active concentration, the drug has to be innocuous for the cell physiology, which might not be an unsurmountable obstacle given the reduced metabolic activity of erythrocytes. However, loading of some antimalarial drugs like clotrimazole had been observed to predispose RBCs to oxidative damage [65], an undesirable scenario since oxidized RBCs are rapidly taken up by hepatic reticuloendothelial system macrophages. Finally, because LPs adsorbed on RBC surfaces would probably sufficiently modify cell shape to target it for removal through spleen filtration, a compromise between stable drug containment and lipid bilayer fusion might have to be reached through the adequate LP formulation, with the objective of achieving LP-RBC merging before spleen removal while avoiding rapid drug leaking from LPs.

5. Conclusion

Antigens found in all RBCs can be a target to consider for antimalarial drug delivery, trading pRBC specificity for a far larger abundance of anchoring points on the cell surface. Because the selected RBC markers are also found on pRBCs, targeted iLPs would have a double activity as therapeutic and prophylactic agents when simultaneously delivering drug to, respectively, infected and non-infected cells. It is reasonable to predict that the nanovector design limitations exposed above can be satisfactorily dealt with, and that some of the future antimalarials yet to be discovered will be harmless for erythrocytes, thus allowing for the loading into them of drug amounts being lethal for *Plasmodium*. If so, the pathogen might encounter its enemy at home, right at the very moment of entering the host cell, which would have devastating effects for the parasite and significantly compromise its survival capacity.

Acknowledgment

This work was supported by grants BIO2011-25039 and BIO2014-52872-R from the Ministerio de Economía y Competitividad, Spain, which included FEDER funds, and by grant 2014-SGR-938 from the Generalitat de Catalunya, Spain. A fellowship of the Instituto de Salud Carlos III (Spain) is acknowledged by P.U. We thank L. D. Shultz and The Jackson Laboratory for providing access to nonobese diabetic scid IL2Rγc null mice through their collaboration with GSK Tres Cantos Medicines Development Campus.

References

[1] K.S. Griffith, L.S. Lewis, S. Mali, and M.E. Parise, Treatment of malaria in the United States: a systematic review, JAMA, 297 (2007) 2264-2277.
[2] World Health Organization, Guidelines for the treatment of malaria, World Health Organization, Geneva, Switzerland, 2010.
[3] P. Newton, Y. Suputtamongkol, P. Teja-Isavadharm, S. Pukrittayakamee, V. Navaratnam, I. Bates, and N. White, Antimalarial bioavailability and disposition of artesunate in acute falciparum malaria, Antimicrob. Agents Chemother., 44 (2000) 972-977.
[4] T.K. Chan, D. Todd, and S.C. Tso, Drug-induced haemolysis in glucose-6-phosphate dehydrogenase deficiency, BMJ, 2 (1976) 1227-1229.
[5] M. Chinappi, A. Via, P. Marcatili, and A. Tramontano, On the mechanism of chloroquine resistance in *Plasmodium falciparum*, PLoS ONE, 5 (2010) e14064.
[6] G. Gregoriadis, Liposomes as a drug delivery system: optimization studies, Adv. Exp. Med. Biol., 238 (1988) 151-159.
[7] A. Singhal and C.M. Gupta, Antibody-mediated targeting of liposomes to red cells in vivo, FEBS Lett., 201 (1986) 321-326.
[8] A.K. Agrawal, A. Singhal, and C.M. Gupta, Functional drug targeting to erythrocytes in vivo using antibody bearing liposomes as drug vehicles, Biochem. Biophys. Res. Commun., 148 (1987) 357-361.
[9] M. Owais, G.C. Varshney, A. Choudhury, S. Chandra, and C.M. Gupta, Chloroquine encapsulated in malaria-infected erythrocyte-specific antibody-bearing liposomes effectively controls chloroquine-resistant *Plasmodium berghei* infections in mice, Antimicrob. Agents Chemother., 39 (1995) 180-184.
[10] P. Urbán, J. Estelrich, A. Cortés, and X. Fernàndez-Busquets, A nanovector with complete discrimination for targeted delivery to *Plasmodium falciparum*-infected versus non-infected red blood cells *in vitro*, J. Control. Release, 151 (2011) 202-211.
[11] D.D. Lasic and F. Martin, Stealth Liposomes. Boca Raton, FL, CRC Press., CRC Press, Boca Raton, FL, USA, 1995.

[12] P. Urbán, J. Estelrich, A. Adeva, A. Cortés, and X. Fernàndez-Busquets, Study of the efficacy of antimalarial drugs delivered inside targeted immunoliposomal nanovectors., Nanoscale Res. Lett., 6 (2011) 620.
[13] A.M. Vaughan, S.H. Kappe, A. Ploss, and S.A. Mikolajczak, Development of humanized mouse models to study human malaria parasite infection, Future Microbiol., 7 (2012) 657-665.
[14] S. Paula, A.G. Volkov, A.N. Van Hoek, T.H. Haines, and D.W. Deamer, Permeation of protons, potassium ions, and small polar molecules through phospholipid bilayers as a function of membrane thickness, Biophys. J., 70 (1996) 339-348.
[15] S. Kyes, P. Horrocks, and C. Newbold, Antigenic variation at the infected red cell surface in malaria, Annu. Rev. Microbiol., 55 (2001) 673-707.
[16] B.M. Cooke, K. Lingelbach, L.H. Bannister, and L. Tilley, Protein trafficking in *Plasmodium falciparum*-infected red blood cells, Trends Parasitol., 20 (2004) 581-589.
[17] K. Kirk, Membrane transport in the malaria-infected erythrocyte, Physiol. Rev., 81 (2001) 495-537.
[18] J.C. Shillcock and R. Lipowsky, Tension-induced fusion of bilayer membranes and vesicles, Nat. Mater., 4 (2005) 225-228.
[19] J.J. Wheeler, L. Palmer, M. Ossanlou, I. MacLachlan, R.W. Graham, Y.P. Zhang, M.J. Hope, P. Scherrer, and P.R. Cullis, Stabilized plasmid-lipid particles: construction and characterization, Gene Ther., 6 (1999) 271-281.
[20] R.C. MacDonald, R.I. MacDonald, B.P. Menco, K. Takeshita, N.K. Subbarao, and L.R. Hu, Small-volume extrusion apparatus for preparation of large, unilamellar vesicles, Biochim. Biophys. Acta, 1061 (1991) 297-303.
[21] G. Stensrud, S. Sande, S. Kristensen, and G. Smistad, Formulation and characterisation of primaquine loaded liposomes prepared by a pH gradient using experimental design, Int. J. Pharm., 198 (2000) 213-228.
[22] H.C. Loughrey, L.S. Choi, P.R. Cullis, and M.B. Bally, Optimized procedures for the coupling of proteins to liposomes, J. Immunol. Methods, 132 (1990) 25-35.
[23] S.M. Ansell, P.G. Tardi, and S.S. Buchkowsky, 3-(2-pyridyldithio)propionic acid hydrazide as a cross-linker in the formation of liposome–antibody conjugates, Bioconjugate Chem., 7 (1996) 490-496.
[24] D.S. Hage, Periodate oxidation of antibodies for site-selective immobilization in immunoaffinity chromatography, Methods Mol. Biol., 147 (2000) 69-82.
[25] N. Maurer, D.B. Fenske, and P.R. Cullis, Developments in liposomal drug delivery systems, Expert Opin. Biol. Ther., 1 (2001) 923-947.
[26] R.C. Switzer III, C.R. Merril, and S. Shifrin, A highly sensitive silver stain for detecting proteins and peptides in polyacrylamide gels, Anal. Biochem., 98 (1979) 231-237.
[27] S.L. Cranmer, C. Magowan, J. Liang, R.L. Coppel, and B.M. Cooke, An alternative to serum for cultivation of *Plasmodium falciparum in vitro*, Trans. R. Soc. Trop. Med. Hyg., 91 (1997) 363-365.
[28] C. Lambros and J.P. Vanderberg, Synchronization of *Plasmodium falciparum* erythrocytic stages in culture, J. Parasitol., 65 (1979) 418-420.
[29] A. Radfar, D. Méndez, C. Moneriz, M. Linares, P. Marín-García, A. Puyet, A. Diez, and J.M. Bautista, Synchronous culture of *Plasmodium falciparum* at high parasitemia levels, Nat. Protoc., 4 (2009) 1899-1915.
[30] P. Urbán, J.J. Valle-Delgado, N. Mauro, J. Marques, A. Manfredi, M. Rottmann, E. Ranucci, P. Ferruti, and X. Fernàndez-Busquets, Use of poly(amidoamine) drug conjugates for the delivery of antimalarials to *Plasmodium*, J. Control. Release, 177 (2014) 84-95.
[31] M. Ramsby and G. Makowski, Differential detergent fractionation of eukaryotic cells, Cold Spring Harbor Protocols, 2011 (2011) rot5592.
[32] P.H. O'Farrell, High resolution two-dimensional electrophoresis of proteins, J. Biol. Chem., 250 (1975) 4007-4021.

[33] I. Angulo-Barturen, M.B. Jiménez-Díaz, T. Mulet, J. Rullas, E. Herreros, S. Ferrer, E. Jiménez, A. Mendoza, J. Regadera, P.J. Rosenthal, I. Bathurst, D.L. Pompliano, F. Gómez de las Heras, and D. Gargallo-Viola, A murine model of *falciparum*-malaria by *in vivo* selection of competent strains in non-myelodepleted mice engrafted with human erythrocytes, PLoS ONE, 3 (2008) e2252.

[34] M.B. Jiménez-Díaz, T. Mulet, V. Gómez, S. iera, A. lvarez, H. aruti, Y. ázquez, A. ernández, J. báñez, M. iménez, D. argallo-Viola, and I. ngulo-Barturen, Quantitative measurement of *Plasmodium*-infected erythrocytes in murine models of malaria by flow cytometry using bidimensional assessment of SYTO-16 fluorescence, Cytometry, 75A (2009) 225-235.

[35] L. Qiu, N. Jing, and Y. Jin, Preparation and in vitro evaluation of liposomal chloroquine diphosphate loaded by a transmembrane pH-gradient method, Int. J. Pharm., 361 (2008) 56-63.

[36] T.D. Madden, P.R. Harrigan, L.C.L. Tai, M.B. Bally, L.D. Mayer, T.E. Redelmeier, H.C. Loughrey, C.P.S. Tilcock, L.W. Reinish, and P.R. Cullis, The accumulation of drugs within large unilamellar vesicles exhibiting a proton gradient: a survey, Chem. Phys. Lipids, 53 (1990) 37-46.

[37] F. Omodeo-Salè, L. Cortelezzi, N. Basilico, M. Casagrande, A. Sparatore, and D. Taramelli, Novel antimalarial aminoquinolines: heme binding and effects on normal or *Plasmodium falciparum*-parasitized human erythrocytes, Antimicrob. Agents Chemother., 53 (2009) 4339-4344.

[38] A. Nair, B. Abrahamsson, D.M. Barends, D.W. Groot, S. Kopp, J.E. Polli, V.P. Shah, and J.B. Dressman, Biowaiver monographs for immediate-release solid oral dosage forms: primaquine phosphate, J. Pharm. Sci., 101 (2012) 936-945.

[39] E. Pachlatko, S. Rusch, A. Müller, A. Hemphill, L. Tilley, E. Hanssen, and H.P. Beck, MAHRP2, an exported protein of *Plasmodium falciparum*, is an essential component of Maurer's cleft tethers, Mol. Microbiol., 77 (2010) 1136-1152.

[40] C. Spycher, N. Klonis, T. Spielmann, E. Kump, S. Steiger, L. Tilley, and H.P. Beck, MAHRP-1, a novel *Plasmodium falciparum* histidine-rich protein, binds ferriprotoporphyrin IX and localizes to the Maurer's clefts, J. Biol. Chem., 278 (2003) 35373-35383.

[41] L. Tilley, G. McFadden, A. Cowman, and N. Klonis, Illuminating *Plasmodium falciparum*-infected red blood cells, Trends Parasitol., 23 (2007) 268-277.

[42] C. Spycher, M. Rug, E. Pachlatko, E. Hanssen, D. Ferguson, A.F. Cowman, L. Tilley, and H.P. Beck, The Maurer's cleft protein MAHRP1 is essential for trafficking of PfEMP1 to the surface of *Plasmodium falciparum*-infected erythrocytes, Mol. Microbiol., 68 (2008) 1300-1314.

[43] J. García, H. Curtidor, O.L. Gil, M. Vanegas, and M.E. Patarroyo, A Maurer´s cleft-associated *Plasmodium falciparum* membrane-associated histidine-rich protein peptide specifically interacts with the erythrocyte membrane, Biochem. Biophys. Res. Commun., 380 (2009) 122-126.

[44] R.J. Howard, S. Uni, M. Aikawa, S.B. Aley, J.H. Leech, A.M. Lew, T.E. Wellems, J. Rener, and D.W. Taylor, Secretion of a malarial histidine-rich protein (Pf HRP II) from *Plasmodium falciparum*-infected erythrocytes, J. Cell Biol., 103 (1986) 1269-1277.

[45] P.D. Siebert and M. Fukuda, Isolation and characterization of human glycophorin A cDNA clones by a synthetic oligonucleotide approach: nucleotide sequence and mRNA structure, Proc. Natl. Acad. Sci. U. S. A., 83 (1986) 1665-1669.

[46] M. Fleiner, P. Benzinger, T. Fichert, and U. Massing, Studies on protein−liposome coupling using novel thiol-reactive coupling lipids: influence of spacer length and polarity, Bioconjugate Chem., 12 (2001) 470-475.

[47] K. Maruyama, T. Takizawa, N. Takahashi, T. Tagawa, K. Nagaike, and M. Iwatsuru, Targeting efficiency of PEG-immunoliposome-conjugated antibodies at PEG terminals, Adv. Drug Deliv. Rev., 24 (1997) 235-242.

[48] P.A. Nygren, M. Eliasson, L. Abrahmsén, M. Uhlén, and E. Palmcrantz, Analysis and use of the serum albumin binding domains of streptococcal protein G, J. Mol. Recognit., 1 (1988) 69-74.
[49] P. Urbán and X. Fernàndez-Busquets, Nanomedicine against malaria, Curr. Med. Chem., 21 (2014) 605-629.
[50] J. Marques, E. Moles, P. Urbán, R. Prohens, M.A. Busquets, C. Sevrin, C. Grandfils, and X. Fernàndez-Busquets, Application of heparin as a dual agent with antimalarial and liposome targeting activities towards *Plasmodium*-infected red blood cells, Nanomedicine: NBM, 10 (2014) 1719-1728.
[51] D. Papahadjopoulos, T.M. Allen, A. Gabizon, E. Mayhew, K. Matthay, S.K. Huang, K.D. Lee, M.C. Woodle, D.D. Lasic, and C. Redemann, Sterically stabilized liposomes: improvements in pharmacokinetics and antitumor therapeutic efficacy, Proc. Natl. Acad. Sci. U. S. A., 88 (1991) 11460-11464.
[52] M. Gulati, M. Grover, S. Singh, and M. Singh, Lipophilic drug derivatives in liposomes, Int. J. Pharm., 165 (1998) 129-168.
[53] V.P. Torchilin, Recent advances with liposomes as pharmaceutical carriers, Nat. Rev. Drug Discov., 4 (2005) 145-160.
[54] V.R. Muzykantov, Drug delivery by red blood cells: vascular carriers designed by Mother Nature, Expert Opin. Drug Deliv., 7 (2010) 403-427.
[55] D.W. Wilson, C. Langer, C.D. Goodman, G.I. McFadden, and J.G. Beeson, Defining the timing of action of antimalarial drugs against *Plasmodium falciparum*, Antimicrob. Agents Chemother., 57 (2013) 1455-1467.
[56] D.M. Harmening, The red blood cell: Structure and function, Clinical Hematology and Fundamentals of Hemostasis, F. A. Davis Company, Philadelphia, PA, 1996, pp. 54-70.
[57] A.L. Bailey and P.R. Cullis, Membrane fusion with cationic liposomes: effects of target membrane lipid composition, Biochemistry, 36 (1997) 1628-1634.
[58] S. Mondal Roy and M. Sarkar, Membrane fusion induced by small molecules and ions, J. Lipids, 2011 (2011) 528784.
[59] I.D. Goodyer, B. Pouvelle, T.G. Schneider, D.P. Trelka, and T.F. Taraschi, Characterization of macromolecular transport pathways in malaria-infected erythrocytes, Mol. Biochem. Parasitol., 87 (1997) 13-28.
[60] S. Loew, A. Fahr, and S. May, Modeling the release kinetics of poorly water-soluble drug molecules from liposomal nanocarriers, J. Drug Deliv., 2011 (2011) 376548.
[61] A. Fahr, P.v. Hoogevest, S. May, N. Bergstrand, and S. Leigh, Transfer of lipophilic drugs between liposomal membranes and biological interfaces: Consequences for drug delivery, Eur. J. Pharm. Sci., 26 (2005) 251-265.
[62] H. Kercret, J. Chiovetti, M.W. Fountain, and J.P. Segrest, Plasma membrane-mediated leakage of liposomes induced by interaction with murine thymocytic leukemia cells, Biochim. Biophys. Acta - Biomembranes, 733 (1983) 65-74.
[63] G. Scherphof, F. Roerdink, M. Waite, and J. Parks, Disintegration of phosphatidylcholine liposomes in plasma as a result of interaction with high-density lipoproteins, Biochim. Biophys. Acta - General Subjects, 542 (1978) 296-307.
[64] J.A. Virtanen, K.H. Cheng, and P. Somerharju, Phospholipid composition of the mammalian red cell membrane can be rationalized by a superlattice model, Proc. Natl. Acad. Sci. U. S. A., 95 (1998) 4964-4969.
[65] I.L. Lisovskaya, I.M. Shcherbachenko, R.I. Volkova, and F.I. Ataullakhanov, Clotrimazole enhances lysis of human erythrocytes induced by t-BHP, Chem. Biol. Interact., 180 (2009) 433-439.